PROTEINS: Structure, Function, and Genetics 1:47–59 (1986)

Focusing of Electric Fields in the Active Site of Cu-Zn Superoxide Dismutase: Effects of Ionic Strength and Amino-Acid Modification

Isaac Klapper,[1] Ray Hagstrom,[1] Richard Fine,[2] Kim Sharp,[3] and Barry Honig[3]

[1]High Energy Physics Division, Argonne National Laboratory, Argonne, Illinois 60439; [2]Department of Biological Sciences, Columbia University, New York, New York 10027, and Department of Structural Biology, Brookhaven National Laboratory, Upton, New York 11973; and [3]Department of Biochemistry and Molecular Biophysics, Columbia University, New York, New York 10032

ABSTRACT **In this paper we report the implementation of a finite-difference algorithm which solves the linearized Poisson-Boltzmann equation for molecules of arbitrary shape and charge distribution and which includes the screening effects of electrolytes. The microcoding of the algorithm on an ST-100 array processor allows us to obtain electrostatic potential maps in and around a protein, including the effects of ionic strength, in about 30 minutes. We have applied the algorithm to a dimer of the protein Cu-Zn superoxide dismutase (SOD) and compared our results to those obtained from uniform dielectric models based on coulombic potentials. We find that both the shape of the protein-solvent boundary and the ionic strength of the solvent have a profound effect on the potentials in the solvent. For the case of SOD, the cluster of positive charge at the bottom of the active site channel produces a strongly enhanced positive potential due to the focusing of field lines in the channel—a result that cannot be obtained with any uniform dielectric model. The remainder of the protein is surrounded by a weak negative potential. The electrostatic potential of the enzyme seems designed to provide a large cross-sectional area for productive collisions. Based on the ionic strength dependence of the size of the positive potential region emanating from the active site and the repulsive negative potential barrier surrounding the protein, we are able to suggest an explanation for the ionic strength dependence of the activity of the native and chemically modified forms of the enzyme.**

Key words: protein electrostatics, substrate diffusion, Poisson-Boltzmann, electrostatic potentials

INTRODUCTION

Electrostatic interactions are believed to play a central role in a variety of biological processes (for recent reviews see references 1–3). However, an accurate description of these interactions has been complicated by serious uncertainties concerning the validity of different treatments as well as by the severe computational requirements that realistic treatments involve. One source of complexity is the large difference in polarizability between any biological macromolecule and the surrounding solvent. This difference implies that electric fields produced by the macromolecule will depend not only on its charge distribution but also on the detailed shape of its surface. As a result, a simple coulombic potential is not valid and any calculation of electrical forces must take the shape of the boundary into account (see Gilson et al.[4] for a discussion of a number of simple cases relevant to proteins and membranes). In addition, when the ionic strength of the solvent is nonzero the potential cannot be obtained by the direct application of Coulomb's law, even for a uniform dielectric, because of the presence of mobile ions in the solvent. There are a number of possible approaches to this problem.

Microscopic approaches based on Monte-Carlo or molecular dynamics simulations treat the macromolecule and solvent at the atomic level and thus the dielectric boundary is not explicitly defined. Rather, the dielectric properties of the macromolecule and solvent are accounted for in terms of molecular charge distributions, polarizabilities, and thermal fluctuations. However, despite dramatic progress in computer simulations of macromolecules and liquids, serious problems still remain in the description of phenomena involving coulombic forces. For the purposes of this work in which we calculate electric fields some distance away from the surface of the macromolecule, an unavoidable problem would be the large number of solvent molecules which would have to be included in any microscopic simulation. Moreover, the effects of free ions within the solvent would be particularly difficult to take into account.

An alternative approach starts from a continuum description of the dielectric properties of the system. The protein is described as a low dielectric medium containing real and partial charges whose coordinates are known from x-ray data. The solvent is de-

Received May 16, 1986; accepted June 17, 1986.

Dr. Isaac Klapper's present address is Courant Institute, New York University, 4 Washington Place, New York, NY 10003.

Address reprint requests to Dr. Barry Honig, Department of Biochemistry and Molecular Biophysics, Columbia University, 630 West 168 St., New York, New York 10032.

© 1986 ALAN R. LISS, INC.

scribed as a high dielectric medium which can contain a simple electrolyte behaving according to Debye-Huckel theory. Electric fields inside or outside the protein are obtained by solving the Poisson-Boltzmann (PB) equation. Analytic solutions are available if the protein is assumed to have a simple shape,[1] but numerical methods are required to treat nontrivially shaped macromolecules. A finite-difference solution to Poisson's equation developed by Warwicker and Watson[5] has been applied to a number of electrostatic problems.[6,7] Zauher and Morgan[9] have recently reported a finite element method which does not solve Poisson's equation directly but obtains induced surface charge at the dielectric boundary. This method was applied to two-dimensional models and preliminary results were reported in three dimensions for lysozyme. The numerical algorithms which have been reported to date have not accounted for the effect of free ions in the solvent.

In this paper we introduce a finite difference algorithm which solves the Poisson-Boltzmann equation for molecules of arbitrary shape and which specifically incorporates the screening effects of the electrolyte. The algorithm is written for a STAR ST-100 array processor with the most time-critical portions written in microcode. The application of the algorithm to the protein Cu-Zn superoxide dismutase (SOD) is reported.

SOD catalyzes the dismutation of the O_2^- radical to O_2 and H_2O_2 in a reaction involving the alternate reduction and oxidation of an active-site copper. The rate constant for the reaction is quite high,[10] approximately an order magnitude lower than the diffusion-limited collision rate of O_2^- with the entire enzyme. Since the reactive target (the copper) is quite small, Koppenol[11] suggested that the substrate is guided into the active site by the electrical field of the protein. This idea gained strong support by the observation of Cudd and Fridovich[12] that increasing the ionic strength decreases the reaction rate. SOD has a net charge of -4, which might be expected to repel the superoxide anion. However, Koppenol[11] suggested that the specific charge distribution of the enzyme, which has a cluster of positive charge near the active site, leads to a net rate enhancement.

A number of investigations of the electrostatic potential of SOD have been made by using pairwise coulombic potentials. Getzoff et al.[13] used a variety of values and distance-dependent expressions for the dielectric constant to demonstrate that the region of the solvent in the vicinity of the active site had a significant positive electrostatic potential. They further argued that repulsive interactions with negatively charged amino acids tended to direct the substrate toward the active site. McCammon and coworkers[14,15] have simulated the diffusion process by using a Brownian dynamics approach. The protein was represented as a sphere and the active site as a reactive patch on the surface of the sphere. Electrostatic interactions were assumed to be coulombic with a uniform dielectric constant of 78 used for both the protein and the solvent. While the simulations did demonstrate that the charge distribution of SOD enhanced the reaction rate relative to that obtained with a charge of -4 placed at the center of the sphere, the calculated rate was still below that obtained for the neutral sphere.[14] The authors point out the need for a proper dielectric model as well as for a more realistic description of the topography of the protein.

In this paper we apply our algorithm to the calculation of electrostatic potentials around a dimer of SOD. We find that both the shape of the dielectric boundary and the ionic strength of the surrounding solvent have a large effect on the shape and magnitude of the calculated field around the protein. By comparing the results to those obtained from a uniform dielectric model, we are able to assess the effect of the shape of the protein on the shape and magnitude of the fields surrounding the protein. We find that the active site crevice of SOD serves to enhance the positive potential of the enzyme by focusing field lines out into the solvent. Basic considerations show that this should have the effect of increasing the rate constant of substrate binding above that predicted by any uniform dielectric model. Results are reported for two different values of the ionic strength and for two chemically modified forms of the protein. The effects of ionic strength on the calculated fields also suggest an explanation for the observed ionic strength effects on the catalytic rates of the native and chemically modified forms of the enzyme.

METHODS

The basic model used to describe the protein and solvent was discussed extensively by Gilson et al.[4] The protein is represented as a low dielectric cavity containing fixed charges and dipoles. The shape of the cavity and the positions of the charges and dipoles are obtained from the crystal structure of the protein. The cavity is assigned a dielectric constant of 2 to account for electronic polarization. The solvent is represented as a medium of dielectric 80 which contains ions that screen the fixed charges according to the Debye-Huckel model.

Poisson-Boltzmann Equation

The electrostatic field around a protein in the presence of salt is estimated by the solution to the linear Poisson-Boltzmann equation

$$\vec{\nabla}\cdot(\epsilon(x)\vec{\nabla}\phi(x)) - \bar{\kappa}^2(x)\phi(x) + 4\pi\rho(x) = 0 \qquad (1)$$

where ϕ is the potential. ϵ is the dielectric constant. ρ is the fixed charge density. κ is the modified Debye-Huckel parameter (which does not include the dielectric constant), given by

$$\bar{\kappa} = \epsilon^{1/2}\kappa = (8\pi e^2 NI/1000kT)^{1/2} \qquad (2)$$

where N is Avogadro's number, e is the proton charge. k is Boltzmann's constant, T is the temperature, and I is the ionic strength. Note that $1/\kappa$ is the Debye screening length and ϕ, ϵ, κ, and ρ are all functions of the vector coordinate, x.

Finite Difference Representation

In the finite-difference method these continuous functions are approximated by distinct values at points on a regular cubic grid of mesh size h. Each value represents an appropriate average of the continuous function over the volume surrounding the given point. For example, the potential at a grid point. ϕ_0 is given by $\iiint\phi(x)d^3x$ over those spatial points which lie closer to grid point 0 than to any other grid point: i.e., the integral is taken over a cube of side h centered on point 0 (Fig. 1). Integrating Eq. (1) over this volume gives

$$\iiint\vec{\nabla}\cdot(\epsilon(x)\vec{\nabla}\phi(x))d^3x - \iiint\bar{\kappa}(x)\phi(x)d^3x - 4\pi\iiint\rho(x)d^3x = 0 \quad (3)$$

We approximate the second integral by $\bar{\kappa}_0\phi_0h^3$ where $\bar{\kappa}_0$ is the value of the modified Debye-Huckel parameter associated with the grid point. The third integral becomes $4\pi q_0$, where q is the total fixed charge inside the volume element. The first term can be transformed to a surface integral using Gauss's theorem, to give

$$\iint\epsilon(x)\vec{\nabla}\phi(x)\cdot d\vec{A} - \bar{\kappa}_0\phi_0h^3 + 4\pi q_0 = 0 \quad (4)$$

where $d\vec{A}$ is the surface normal vector representing the area of the cube. A forward finite difference formula for the grad operator in the first term in Eq. (4) gives

$$\int\epsilon\vec{\nabla}\phi\cdot d\vec{A} = \Sigma\epsilon_i(\phi_i - \phi_0)h \quad (5)$$

where ϕ_0 is the potential at the grid point, ϕ_i (i = 1–6) is the potential at the six neighboring grid points in the positive and negative directions along the x, y, and z axes, respectively, and ϵ_i is the dielectric constant associated with the center of the square faces bounding the volume element, i.e., at the center of each grid line joining the point to its neighbors (see Fig. 1). Thus Eq. (3) becomes

$$h\Sigma\epsilon_i(\phi_i - \phi_0) - h^3\bar{\kappa}_0^2\phi_0 + 4\pi q_0 = 0 \quad (6)$$

Rearranging Eq. (6) and solving for ϕ_0 gives the required difference equation:

$$\phi_0 = \frac{(\Sigma\epsilon_i\phi_i + 4\pi q_0)}{(\Sigma\epsilon_i + \bar{\kappa}^2h^2)} \quad (7)$$

Equation (7) is solved by making an initial guess of ϕ at all the grid points calculating new estimates by using Eq. (7) and updating the value of ϕ everywhere (Jacobi relaxation[16]). This is repeated until the mean square change in successive iterations is less than a preset value, typically 0.0001.

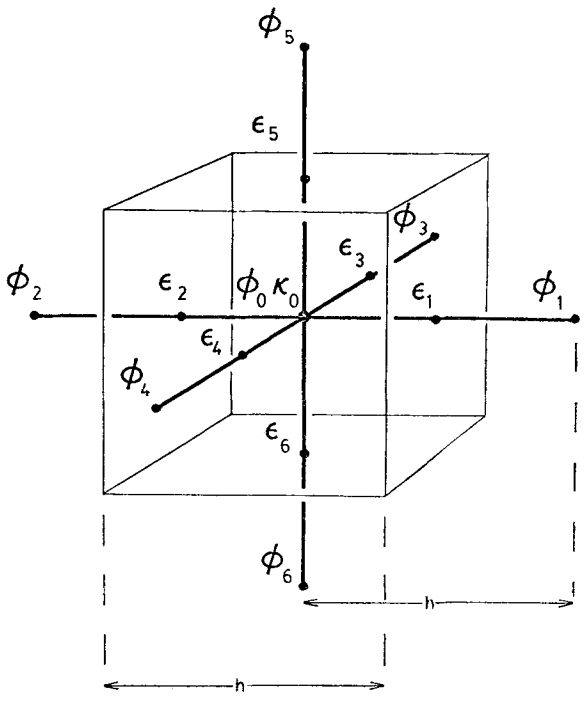

Fig. 1. Cubical volume element associated with a grid point (subscript 0). Grid lines that join neighboring points are shown in bold. Associated with the midpoint of each line is a value for the dielectric constant, ϵ. The potential ϕ, and the Debye-Huckel parameter, κ are associated with the center of the cube. The grid spacing is h.

Implementation on Array Processor

In order to accurately represent the surface of the protein it is desirable to have the finest possible grid. However, the solution time will increase at least as the cube of the grid size, requiring very fast computational techniques. Fortunately finite-difference equations can conveniently be vectorized, allowing efficient computing hardware such as array processors to be used. To implement Eq. (7) on an ST-100 array processor we divided a cubical box into a $65\times65\times65$ grid, this being the largest grid of order $2^n + 1$ that could be accommodated by the architecture of the machine. The algorithm was written in ST-100 Array Processor Control Language (APCL) with the exception of the most time-critical portions, which were written in microcode.

To speed up convergence a technique called multigridding is used. This involves solving the equation on a coarse grid, using the results to provide a smart initial guess (by linear interpolation) for the potentials on a new grid twice as fine, and solving the equation on the new grid. This procedure is started on a $3\times3\times3$ grid and repeated on successively finer

grids until the final grid size is $65\times65\times65$. This results in more rapid convergence since the iterations on the finest grid, which consume most of the time, start with a reasonable approximation to the final solution.

For the applications discussed in this paper, typical runs required about 30 minutes elapsed time on a VAX 11/780-ST-100 system which included about 15 minutes of ST-100 central processing unit (cpu) time. This represents a speed up over the VAX of a factor of about 30 and compares with a benchmark of 8–10 minutes on a Cray 1 reported by Rogers and Sternberg,[8] for a smaller grid of $60\times60\times60$, without the ionic strength term in Eq. (7). In comparing this time to that of Rogers and Sternberg, it should also be noted that in order to produce a finer representation of the dielectric boundary, we assign a value for the dielectric for each grid line, rather than each grid point. This requires three times as many values, which thus increases the time per iteration somewhat. The other method used for calculating electric fields numerically that has been applied to proteins is the finite element method.[9] However, it is difficult to make a direct quantitative comparison with this method since no calculation times are given. In addition there appears to be no way to incorporate the contribution of electrolyte ions in this method.

Boundary Conditions

The points at the outer boundary of the box have ϕ specified and these potentials are not relaxed, retaining their initial values. This corresponds to the application of Dirichlet boundary conditions.[17] Boundary values are either set to zero or calculated from the Debye-Huckel expression

$$\phi_i = \Sigma(q_j e^{-\kappa r_{ij}})/80 r_{ij} \qquad (8)$$

where r_{ij} is the distance of the jth charge from the ith grid boundary point. This expression approximates the analytical solution far from the protein and is a better approximation to the correct boundary values than zero under most conditions.

Modeling Proteins

A FORTRAN program has been written to map the atomic coordinates of a protein, taken from Brookhaven Protein Data Bank, onto our grid. The center of coordinates of the protein is placed at the center of the box. The coordinates of the protein are scaled such that the maximum linear dimension of the protein corresponds to a predetermined fraction of the side of the box. The charge on each charged atom is represented by assigning fractional charges to the nearest eight grid points by using a trilinear weighting function. This preserves the maximum number of moments of the original charge distribution. The fraction of the charge, f, assigned to a grid point is given by

$$f = (1-a)\cdot(1-b)\cdot(1-c) \qquad (9)$$

where a, b, and c are the distances of the charge from the grid point in the x, y, and z directions, respectively, expressed as a fraction of the grid spacing h.

The protein-solvent boundary is determined as the solvent accessible van der Waals surface by the method of Connolly.[18] Then ϵ at each dielectric point in the grid (see Fig. 1) is assigned a value of either 2 or 80 depending on whether it is inside or outside the protein. κ is set to zero for grid points in the interior of the protein and to the bulk value outside. In cubical volume elements partially occupied by protein, the value of κ at the center is the mean of the values determined at the six midpoints of the associated grid lines.

In this work, the longest linear dimension of SOD dimer is scaled so that it occupies two-thirds of the side of the box. This insures that the protein is surrounded by enough bulk solvent so that the potential at the boundary of the grid is close to zero or can be adequately calculated from Eq. (8). The longest linear dimension of SOD is about 65 Å,[19] and thus the grid spacing is about 1.5 Å and the dimension of the box is 95 Å. This implies that there is a minimum of 15 Å (about 2 Debye lengths at physiological ionic strength) of bulk solvent separating the protein and the edge of the box. It may, in general, be possible to decrease the volume of solvent and thus improve the resolution of the calculation at the surface of the protein but this must be carefully considered in each application.

Charges were assigned to the atomic coordinates of SOD[19,20] as follows: the ϵ nitrogen of each lysine, +1; each guanidinium nitrogen, +.5; each carboxylate oxygen, −.5. All histidines were assumed to be neutral except His-41 and His-61. His-41 was assigned a charge of +1 and His-61 of −1, as discussed previously.[13,15,19] The charge on these two histidines was split between the two ring nitrogens. The Cu and Zn were assigned a charge of +2 as in the oxidized enzyme. Partial charges were assigned according to reference 21.

RESULTS

Accuracy of the Algorithm

Several test cases with analytical solutions were solved to gauge the accuracy and precision of the method by using grid sizes of about 1 Å.

Single ion with/without salt

With Eq. (8) as a boundary condition the solution is accurate to $<3\%$ everywhere except at the grid point where the charge is placed where the analytical solution has a singularity. This accuracy is obtained both without salt (infinite Debye length) and with salt (Debye length of 8 Å). With a zero boundary

condition the solution is also accurate to <3% everywhere except within 5 grid units from the edge of the grid where, due to the imposed boundary condition, the numerical solution becomes increasingly small compared to the analytical solution.

Dipole in cavity with/without salt

A dipole consisting of two charges, magnitude 4e separated by 1.5 Å was placed in the center of a spherical cavity of dielectric 2, radius 50 Å surrounded by dielectric 80. The diameter of the sphere was two-thirds the size of the grid. With Eq. (8) as a boundary condition the solution is accurate to <3% everywhere except close to the charges where the analytical solution is singular, and at the dielectric boundary (Fig. 2). At the grid point closest to the dielectric boundary, the numerical solution had an error of about 25%, dropping to 5% at the neighboring grid points. The accuracy of the solutions is similar with and without salt in the solvent. Addition of salt has little effect on the potential in the low dielectric region except for grid points 1 or 2 grid units from the dielectric boundary.

In further work we have found that it is possible to achieve an accuracy of <1%, even for the more complicated case of a point charge embedded in a sphere in a uniform electric field. However, in order to achieve this accuracy it is necessary to utilize a modified method we have developed for the assignment of the dielectric constant. This involves numerically integrating over those volume elements in the grid which are partially occupied by the low dielectric sphere. This method is quite time consuming and is unnecessary for the applications described in this paper.

Application to Superoxide Dismutase

Effect of dielectric model

Figure 3 displays contour maps of electrical potential obtained from the application of three different dielectric models to SOD in the absence of salt. Contour maps are shown for a slice through the active site. While the dimeric nature of the protein is evident from the maps, there is a clear absence of true symmetry due to differences in the crystal structures of the two monomers.

Figure 3a is obtained from a uniform dielectric model with $\epsilon=80$; that is, the potential at any point is simply the sum of all the coulombic potentials of the real charges in the protein. The figure indicates that the net negative charge on the protein dominates the electrical potential except in the immediate vicinity of the active site where the cluster of positive charge produces the largest interactions. There is a clear "window" for the substrate to reach the active site channel but the attractive force on the superoxide anion is not appreciable except near the base of the channel. The 1-kT contour extends out about 8 Å from the copper (column 2, Table I).

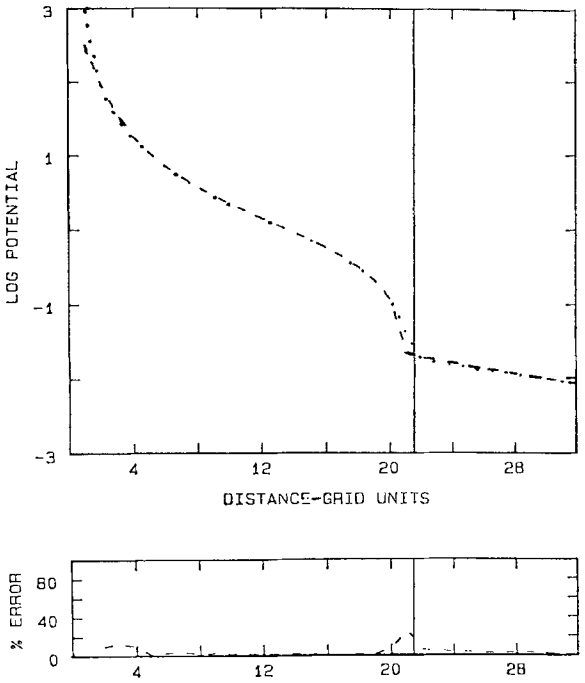

Fig. 2. Comparison of analytical and numerical solutions for the case of dipole at the center of a 20-Å radius sphere, dielectric 2, surrounded by a medium of dielectric 80, with infinite Debye length. Top panel is a semilog plot of the potential vs. distance away from the dipole along the dipole axis (1 Å/grid unit). The dielectric boundary is indicated by the vertical line. The dotted line is the analytical solution. The potential is in units of kT. Lower panel shows the difference between the numerical and analytical solutions, expressed as a percentage of the analytical value.

The contours in Figure 3b are obtained by using a uniform dielectric model with the distance-dependent dielectric constant of $\epsilon=R$, where R is the distance from a particular charge. This is one of the models used in the calculations of Getzoff et al.[13] In this case, the 1-kT positive contour extends out into the solvent about 23 Å from the copper, much further than in Figure 3a. The negative contours also extend further, because the dielectric constant is less than 80 for all interactions within the grid. Negative potential is again found to dominate and there is an appreciable repulsive potential surrounding the protein. It should be pointed out that the distance-dependent dielectric model was developed to describe interactions within the protein and is clearly incorrect for interactions in the high dielectric solvent.

Figure 3c displays results obtained from our linearized Poisson-Boltzmann algorithm at infinite Debye length (zero ionic strength). The effects of protein shape can best be determined by comparing Figure 3c to Figure 3a since the dielectric constant of the solvent is set to 80 in both cases. The difference is that in Figure 3a the protein also has a dielectric constant of 80 while Figure 3c was obtained by assigning the protein a dielectric constant of 2. As is

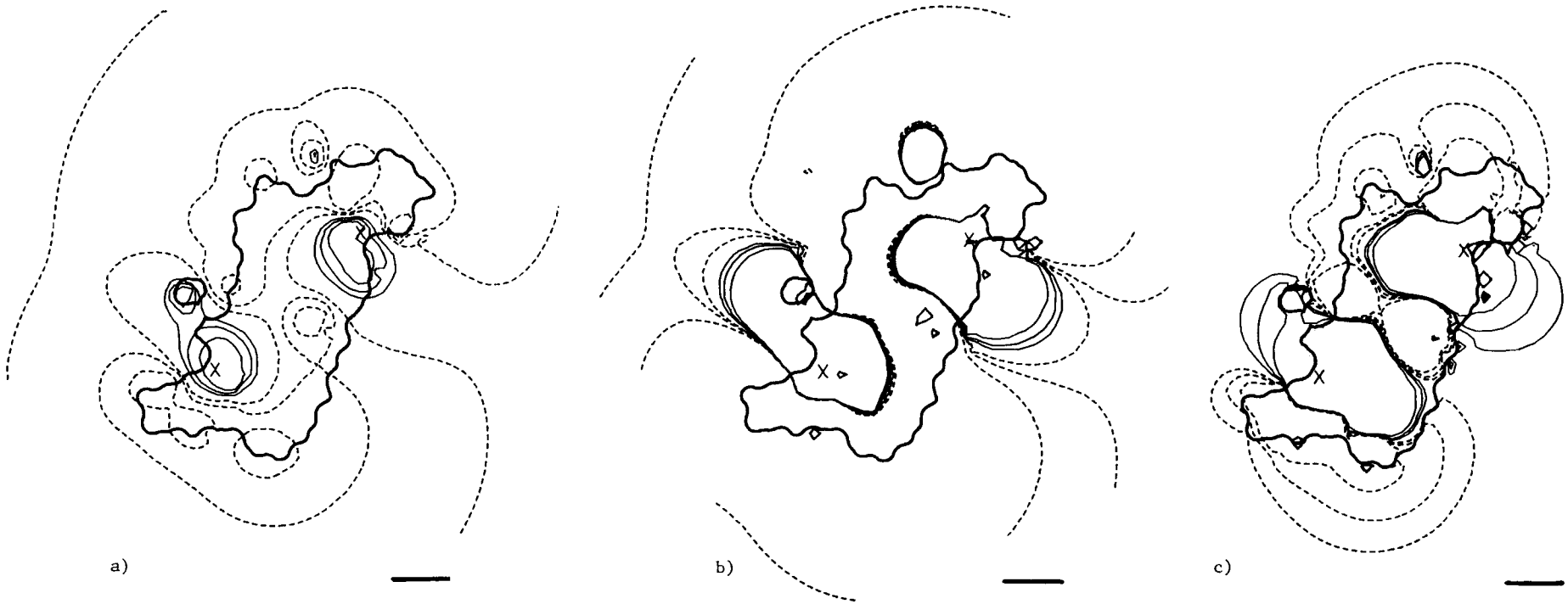

Fig. 3. The electrostatic potential produced by the real charges in superoxide dismutase (SOD) in a two-dimensional slice through the active site region. Contour levels of kT/2, 1kT, and 2kT are given. Negative potential is represented by dashed lines and positive potential by solid lines. The surface of the protein is represented by a heavy solid line. The copper position is marked by an X. The line at the lower right denotes 10 Å. The contours were obtained from a) a uniform dielectric model with a dielectric constant of 80 everywhere, b) a uniform dielectric model with a distance-dependent dielectric constant of $\epsilon = R$, c) the numerical solution obtained from Eq. (7) at infinite Debye length.

TABLE I. Enzyme Activity and Electrostatic Target Features*

Potential map	Enzyme activity† (%)	Contour distance (Å) 2 kT	Contour distance (Å) 1 kT	Target contour area (Å^2) 2 kT	Target contour area (Å^2) 1 kT	Barrier height (kT)
Uniform dielectric of 80 (Fig. 3a)	—‡	5	8	1,050	1,850	0.7
Distant-dependent dielectric (Fig. 3b)	—‡	22	23	2,300	2,600	1.6
Two-dielectric no salt (Figs. 3c and 4a)	100	12	17	2,100	3,100	0.14
Two-dielectric plus salt (Fig. 4b)	60	9	12	2,000	2,400	0.007
No Arg-141 no salt (Fig. 4c)	22	8	11	2,100	2,750	0.25
No Arg-141 plus salt (Fig. 4d)	6	7	8	2,100	2,250	0.009
No lysines no salt (Fig. 4e)	5	6	6	1,850	1,850	2.54
No lysines plus salt (Fig. 4f)	22	6	8	1,900	1,900	0.37

*Areas were obtained by digitizing three-dimensional contour maps. The error in the quoted figures is about 10%. Approximate distances of contours from the copper were taken along a line through the center of the active site cleft and are given for comparison. Barrier heights were obtained by searching for saddle points in the three-dimensional map and are accurate to about 5%. For a description of the terms target contour area and barrier height see Discussion.

†Activity is expressed as a percent of that for the native enzyme in the absence of salt. Data is taken from reference 12.

‡Not applicable.

evident from Figure 3a and 3c, the shape of the protein has a significant effect on the electrical potential. The positive contours extend much further out into the solvent than they do in the uniform dielectric model while the negative contours remain much closer to the protein. Perhaps the most dramatic effect is the ballooning out of the positive contour lines from the active site channel. For example, the 1-kT contour line is approximately 10 Å further from the bottom of the channel in Figure 3c than it is in Figure 3a (Table I). The effect may be viewed as resulting from a focusing of field lines in the high dielectric channel. This effect could not be produced by any uniform dielectric model since in such cases the field lines spread out evenly in all directions. The existence of "cleft potentials" has been noted in previous studies where numerical methods were used to solve the Poisson equation for a protein.[7,9]

Effect of ionic strength and selective modification of charged residues

Figure 4 displays the results from the application of our algorithm to SOD by using a protein dielectric of 2 and a solvent dielectric of 80 ·with no salt (zero ionic strength) and with salt (physiological ionic strength, Debye length = 8 Å) for the native enzyme and two amino-acid-modified forms.

Figures 4a and 4b display the electrical potential around SOD calculated without and with salt, respectively. On increasing the ionic strength the contour lines contract toward the protein surface, as expected, the 1-kT positive contour moving about 5 Å closer to the copper (Table I). At physiological ionic strength and with the 1-kT contour level as a guide the protein would appear neutral to any charged particle more than 4 Å away, except around the active site, where the positive contour still extends about 12 Å from the copper.

As pointed out in the beginning of this paper, the decrease of superoxide dismutase activity with increasing ionic strength[12] provides direct experimental evidence for electrostatic guidance of the substrate into the active site. When the ionic strength is increased from 0 to 130 mM the catalytic activity drops by 40% (column 1, Table I). Cudd and Fridovich[12] showed that acetylation of the lysine residues of SOD, eliminating their charge, changes the catalytic activity at 0 mM by >90%, but when the ionic is increased to 130 mM the activity *increases* to 20%. When a single arginine, Arg-141, is modified with phenylglyoxal, the activity in the absence of salt is reduced to 20% of that of the native enzyme. However, by contrast to the lysine modification, the activity decreases to 6% at 130 mM ionic strength. Since only the modification of the lysines reverses the ionic strength dependence it was concluded[12] that these residues are important in providing electrostatic guidance, while Arg-141 plays a catalytic role rather than a direct role in binding. In order to address these observations, we have calculated the electrostatic potential of SOD with all the lysines neutral and with only Arg-141 neutral, for a Debye length of ∞ and 8 Å (Fig. 4c–f). The electrostatic potential of the Arg-141-modified protein is found to be very similar to the native enzyme although the positive contour lines near the active site are contracted somewhat, particularly at infinite Debye length. In contrast, the electrostatic potential of the lysine-modified protein is modified in two ways: the positive potential near the active site is reduced relative to the native enzyme while the negative potential surrounding the entire protein is enhanced. Moreover, at infinite Debye length there is a barrier of negative potential inhibiting the penetration of substrate to the active site channel. It is, of course, hardly surprising that modification of a single arginine has a smaller effect than modifying ten lysines.

a)

b)

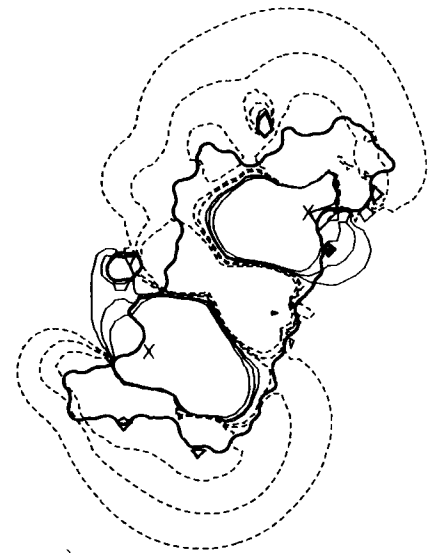

c)

d)

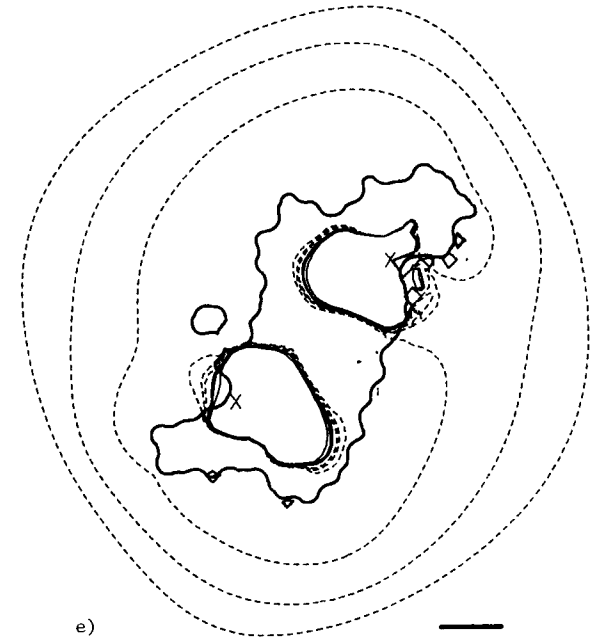

e)

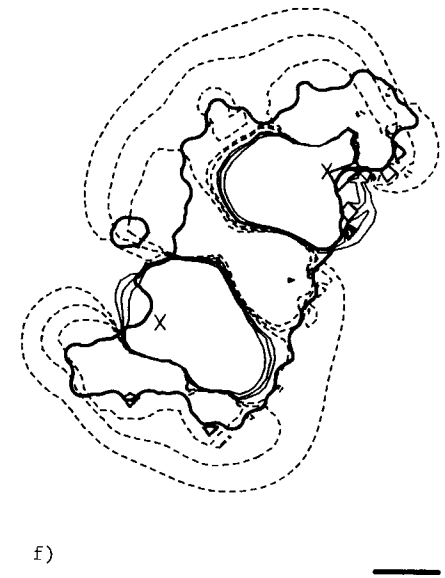

f)

Figures 3 and 4 represent a single slice through the protein. We have plotted contour lines in many slices perpendicular to different axes and the trends remain the same. The protein has a large region of positive potential emanating from the active site while the remainder of the surface is negative, both with no salt and at physiological ionic strength. This can be clearly seen in the three-dimensional plots shown in Figure 5.

Tests of assumptions

We have carried out a series of calculations in order to test the sensitivity of our results to a number of the uncertainties in our description of both the protein and the solvent. Calculations were carried out with bound waters included as part of the protein and by increasing the van der Waals radius of each atom by 1.5 Å. These calculations were intended to test the sensitivity of our results to the detailed description of the dielectric boundary. Thus, increasing the van der Waals radius of each atom extends the low dielectric region out into the solvent and is equivalent to defining a boundary layer of low dielectric solvent molecules. The effect on the potentials in the solvent was quite small (a few percent) although obviously the potentials at the dielectric boundary were markedly altered. Increasing the dielectric constant of the protein from 2 to 4 also had only a few percent effect on the potentials in the solvent.

Finally, we have carried out calculations which included all the partial charges on the protein as well as the real charges which are responsible for the potentials shown in Figures 3–5. While partial charges have a large effect on the potentials in the interior of the protein, the dipolar potential of the partial charges dies out quite quickly in the solvent and has little effect on the patterns illustrated in Figures 3–5.

DISCUSSION

We have described the implementation of an efficient finite-difference algorithm on an ST-100 array processor which solves the linearized Poisson-Boltzmann equation for molecules of arbitrary shape and charge distribution in the presence of an electrolyte solution. In this study we have applied the algorithm to the calculation of electrostatic potentials around SOD and shown that both the detailed shape of the surface of the protein and the ionic strength have large effects on the shape and magnitude of the electric field surrounding the protein. We now consider the significance of these effects for the diffusion of the substrate to the active site of SOD.

Diffusion of the superoxide ion to a sphere representing SOD in a uniform dielectric has been discussed by Allison et al.[14] and a good review of the theory of diffusion is given by Berg and Von Hippel.[22] The diffusion-controlled rate of association of a small substrate diffusing to a target patch on a sphere in the absence of long range forces is proportional to the linear dimension of the patch. For a circular patch, the rate is proportional to $R \cdot \sin \theta/2$, where R is the sphere radius and θ is the half angle subtended by the patch. However, in the presence of long-range forces, the situation is more complex. Superoxide dismutase has a net charge of -4, and the substrate has a charge of -1. In the absence of salt, far from the protein the substrate will experience only the monopole field of the protein and is repelled by it. Thus there is always a barrier to the diffusion of the substrate to the active site, even though closer to the active site there may be an attractive potential. In the presence of salt, there may be directions of approach for which the field of the protein is attractive at all distances. For the case of SOD, no such direction was found; however, the repulsive barrier was found to be substantially reduced.

A quantitative estimate of the association rate can be obtained from our field maps by using Brownian dynamics—work which is currently underway. However, even without such simulations, it is possible to infer how changes in the field maps will affect the diffusion. Clearly important factors controlling the association rate are the size of the target area and the height and width of the barrier that the substrate has to cross to reach the active site.

In the Brownian simulations of Allison et al.[15] the target size was taken to be a circular patch of 10° on a 30-Å sphere, which corresponds to a target area of about 180 $Å^2$, 1.5% of the total area. In a simulation of the diffusion of the substrate to the copper an operational definition of the target area may be taken to be that region of solution surrounding the active site from which the probability of the diffusing particle escaping is small. For the purposes of discussion we use two different estimates of the target patch size as the solution portions of the 2-kT and 1-kT contours surrounding the copper, since in this region the substrate must cross an energy barrier of at least 2 kT or 1 kT to escape. For the maps shown in Figures 3 and 4, the approximate distances from the copper atom to these contours along a line through the center of the active site cleft, as well as the target size defined by the surface area of the contours, are given in Table I, columns 2–5. It should be remembered throughout the following that, although we define and discuss the size of target patches in terms of their areas, the theoretical diffusion-controlled rate of as-

Fig. 4. The electrostatic potential of SOD obtained from Eq. (7) in a two-dimensional slice through the active site region. Contour levels of kT/2, 1kT, and 2kT are given. Negative potential is represented by dashed lines and positive potential by solid lines. The surface of the protein is represented by a heavy solid line. The contours were obtained from (a) all the real charges in SOD at $1/\kappa = \infty$, (b) all the real charges in SOD at $1/\kappa = 8$ Å, (c) same as a but Arg-141 neutral, (d) same as b but Arg-141 neutral, (e) same as a but all lysines neutral, (f) same as b but all lysines neutral.

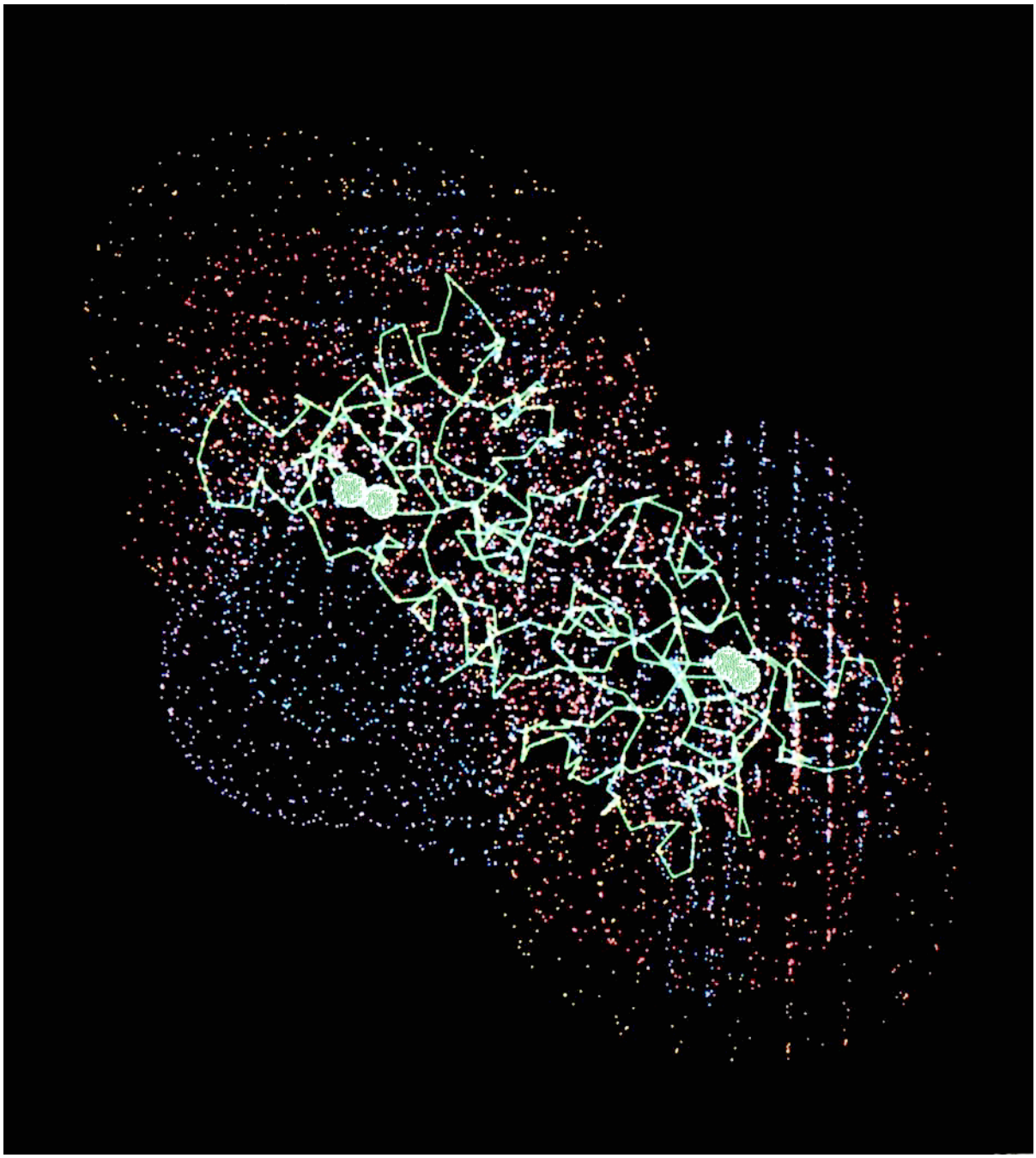

Fig. 5. 1/2kT contours of electrostatic potential around SOD. Contours are for both $1/\kappa = \infty$ and $1/\kappa = 8$ Å. For $1/\kappa = \infty$, positive potential is purple, negative is gold. For $1/\kappa = 8$ Å, positive is blue, negative is red.

sociation for different-sized patches of constant shape would be expected to depend on a suitably defined linear dimension, such as the square root of the area.

For the case of a spherically symmetrical repulsive interaction around a sphere of radius R, the effective radius R* is given by[22]

$$1/R^* = \int r^{-2} e^{U(r)/kT} dr \qquad (10)$$

where U(r) is the potential as a function of the radial coordinate r, and the limits of integration are from R to ∞. It should be noted that the integrand contains the exponential of the potential function and that the effective target radius decreases as U(r) increases. Since neither SOD nor the potentials surrounding it are spherically symmetric the calculation of an effective radius would require a weighted integral over all

paths to the protein, which could only be done by using numerical methods. However, to illustrate the effect of the repulsive barrier, consider the case of a 30-Å sphere surrounded by a spherical barrier of height 1 kT, thickness 10 Å. Equation (10) gives an effective radius of 21 Å. If a barrier height of 2 kT, thickness 5 Å is used instead, the effective radius is reduced to 16 Å. These size barriers are similar to those appearing in the maps for the distance-dependent dielectric model (Fig. 3b) and the lysine-modified protein at zero ionic strength (Fig. 4e). If we integrate the actual repulsive potential profile from the map in Figure 3b along a ray from the copper through the center of the active site cleft, we obtain a reduction in effective radius from 30 Å to 19 Å while the potential profile from the map of Figure 4e gives an effective radius of only 9 Å. Since the diffusion-controlled rate of association is proportional to the effective radius,[22] it is clear that barrier heights above 1 kT have a large effect. The minimum negative potential barrier that the superoxide ion has to cross to reach the target patch for each of the potential maps is given in column 6, Table I.

Effect of Dielectric Model

Based on the contours of Figure 3a, the protein's electrical potential produced by a uniform dielectric model with $\epsilon=80$ would not seem to account well for the high collision rate with the active site copper. (Recall that the fundamental problem in SOD is to account for the fact that the substrate finds the active site copper in times that are only an order of magnitude lower than the diffusion-limited collision rate with the entire protein.) Although there is an attractive region in the vicinity of the active site the target area is relatively small, about 1,050/1,850 $Å^2$ (for 2 and 1 kT, respectively, Table I). In addition the channel barrier is significant at 0.7 kT.

In the distance-dependent dielectric model (Fig. 3b) the target area is much larger (2,300/2,600 $Å^2$) but the entire protein is surrounded by a larger negative potential which poses a 1.6-kT barrier to the diffusion of the substrate to the active site.

The potential produced in the two dielectric model (Fig. 3c) is clearly more favorable for substrate binding than either of the other two potentials. An attractive region emanates from the active site, providing a larger target area of 2,100/3,100 $Å^2$. The channel barrier is also only 0.15 kT. The negative potential is limited to regions of the surface which would not be expected to interfere with the substrate finding the active site. With a protein surface area of about 6,000 $Å^2$,[19] the effective target area as defined here is 25–30% of the protein area compared to the figure of 10% suggested by Getzoff et al.[13] based on the area of the active site cleft. The repulsive regions might help avoid unfavorable binding while remaining weak enough not to repel the substrate from the general vicinity of the protein. In this way, two-dimensional diffusion of the substrate and perhaps rotational diffusion of the protein can ensure a high probability of the substrate finding the active site.

Effect of Ionic Strength

In the two-dielectric model the overall shape of the potential map remains the same when the ionic strength is increased from zero to physiological (Fig. 4a,b). The mobile ions effectively screen the monopole potential of the protein at long range, and the barrier potential, although low with no salt, is decreased even further, to less than 0.01 kT, tending to increase the activity. Opposing this increase, however, is a substantial (30% at the 1-kT level) decrease in the target area. Since even the 1/2-kT contour does not extend much further than 10 Å from the protein surface, the diffusing substrate first encounters the electrostatic field of the protein close to the surface, where that field is dominated by the local shape and charge distribution. Perhaps the best characterization of this map is that of a weakly repulsive potential in most regions of the protein with two attractive "sticky patches" around the active sites.

Effect of Amino-Acid Modification

The main effect of Arg-141 modification is to decrease the attractive potential somewhat in the vicinity of the active site. There is less than a 10% decrease in the target area. However, the barrier height in the absence of salt, although small, is nearly doubled on modification of the arginine, suggesting that this residue does somewhat enhance the catalytic rate electrostatically, as well as chemically, contrary to previous suggestions. That this effect is not large enough to reverse the ionic strength dependence of the activity is indicated by the overall similarity of the potential maps (Fig. 4a,b and 4c,d). The changes in both target area and barrier height with ionic strength for both the native and arginine-modified enzyme are very similar (Table I), thus allowing us to infer that the activity of the Arg-141-modified protein has the same ionic strength dependence as that of the native enzyme, which is consistent with the experimental observations.

The effect of lysine modification is larger than that of the Arg-141 modification since many more charges are involved. With no salt the effect is to increase the barrier height substantially from 0.15 to 2.5 kT and to decrease the target area at the 1-kT level by nearly a factor of 2. Both these effects would be expected to significantly decrease the activity, as is observed experimentally.[12] Increasing the ionic strength has a dramatic effect on the shape of the potential of the modified protein. The negative potential is reduced around the entire protein, and while the target area is unaffected, the barrier height is reduced to 0.14 kT. These changes, which are graphically shown in Figure 4e and f, thus suggest a clear explanation of why the activity increases with increasing ionic strength in the lysine-modified enzyme. In contrast, the decrease in activity of the native enzyme with ionic

strength appears due to the decrease in effective target area. Lowering the barrier height in the native enzyme has a smaller effect on increasing the activity since the barrier is already very low.

Finally, it should be noted that direct comparisons of the activities of the Arg- and Lys-modified proteins cannot be made on the basis of target areas and barrier heights alone since Arg-141 is likely to play a catalytic role in addition to any effect it may have on substrate diffusion.

Possible Sources of Error in Field Determination

It is important to consider possible sources of error in our calculations. It is first worth emphasizing that within the limitations of the model, our solutions are correct to within a few percent. However, the basic assumptions of the model need to be carefully evaluated. One source of uncertainty concerns our treatment of the solvent. For example, it is possible that ordered water at the protein surface has a lower value of ϵ than bulk water. We tested this possibility by increasing the radius of each atom in the protein by 1.5 Å. This is the equivalent of assuming a boundary layer of water having a dielectric constant of 2. As mentioned above, this had little effect on the electrical potential in the solvent.

A second area of concern is our use of the linearized Poisson-Boltzmann equation to treat the electrolyte. While the linear approximation is probably adequate for bulk solvent, the large cleft potential leads to a buildup of charge in the channel, leading, for example, to a concentration of anions of approximately 3 M about 6 Å from the copper, and much larger concentrations of anions at the base of the channel. This physically unrealistic concentration results from the enormous positive potential produced by the cluster of positive charge at the bottom of the channel. However, at high concentrations the assumption of linearity clearly breaks down and thus the expected concentration of ions is probably much smaller than we calculate. Moreover, it is possible that image effects would reduce the concentration of ions in the narrow regions of the channel. It thus appears that we are overestimating the screening effects of the electrolyte in the channel, but not around the rest of the protein. The fact that the cleft potential is significant even when the screening effect is overestimated is a strong indication that this phenomenon is a real one. In order to test the possible effect of an unrealistically large concentration of counter ions at the base of the channel the radius of the copper was increased artificially to 6 Å so as to exclude ions from its immediate vicinity. The potential contours remained essentially unchanged.

SUMMARY

We have calculated the electrostatic potential around SOD for three different dielectric models and at two different ionic strengths for both the native and two amino-acid modified proteins. The choice of dielectric model has a large effect on the potential. For both the uniform dielectric of 80 and the distant-dependent dielectric model, the region of positive potential around the active site is restricted in extent and surrounded by an appreciable negative potential. In contrast, when the two-dielectric model is used, with a protein dielectric of 2–4 and a solvent dielectric of 80, the characteristics of the potential map are altered. The positive region around the active site extends further into the solvent, and the negative barrier is reduced. This focusing of the positive potential is due to the existence of two dielectric regions, which results in concentration of field lines in the higher dielectric medium. This effect is enhanced when charges are close to the dielectric boundary[4] and in clefts, as is the case for the copper and zinc atoms in SOD. Thus in this model the shape of the protein, as well as the charge distribution, is important in determining the field.

Our method also permits, for the first time, the calculation of ionic strength effects on the potential map of an irregularly shaped protein such as SOD. Increasing the ionic strength contracts the potential contours toward the protein surface, as expected. The effect on the negative contours is proportionally greater, since the solvent ions screen the monopole potential more effectively than the higher-order multipoles. The consequences for diffusion of the substrate to the active site copper are that increasing the ionic strength results in a smaller negative potential barrier around the protein and a smaller positive region to form a target for the diffusing substrate. A reduced potential barrier will increase the substrate/enzyme association rate, while the reduced target area will decrease it. The net rate will depend on the balance between these two opposing factors and could thus increase or decrease with ionic strength. We want to stress that the exact rate cannot be calculated from these two parameters alone, but that they show the essential features of these potential maps. This work suggests that the effective target area for diffusion of the substrate to SOD may be larger than previously supposed, and that changes in the effective target size with ionic strength must be considered when calculating the diffusion rates. The two-dielectric model best explains the high experimental association rate since it results in both a large target area and a low repulsive barrier. Moreover, although the opposing effects of target size and repulsive electrostatic barrier may be subtle, the overall effect in the case of the lysine-modified protein is clear, and allows us to suggest an explanation for the reversal in ionic strength dependence of activity upon modification.

The overall picture that these potential maps suggest is that the electrostatic field of SOD does not really guide the substrate into the active site but rather has been designed to allow the superoxide anion to find the large cross-sectional area of the

active site without being repelled by the net negative charge of the protein. The regions of negative potential do not direct the substrate toward the active site (except in its immediate vicinity) but may play a role in preventing unproductive collisions between the enzyme and substrate. In contrast, it seems clear that the cleft potential produced by the cluster of positive charge in the active site plays a crucial role in providing a large target area for the substrate.

ACKNOWLEDGMENTS

We thank Cyrus Levinthal and Michael Gilson for many helpful discussions. This work was supported by grants from Star Technologies and ANL Exploration R&D Fund (R. Hagstrom), NIH-GM30518 and NSF-DMB85-03484 (B. Honig), NIH-P41 RR00442 (C. Levinthal), and DE/AC02/72 (B. Schoenborn).

REFERENCES

1. Matthew, J.B. Electrostatic effects in proteins. Annu. Rev. Biophys. Biophys. Chem. 14:387–417, 1985.
2. Warshel, A., Russell, S.T. Calculation of electrostatic interactions in biological systems and in solution. Q. Rev. Biophys. 17:283–422, 1985.
3. Honig, B., Hubbell, W., Flewelling, R. Electrostatic interactions in membranes and proteins. Annu. Rev. Biophys. Biophys. Chem 15:163–193, 1986.
4. Gilson, M., Rashin, A., Fine, R., Honig, B. On the calculation of electrostatic interactions in proteins. J. Mol. Biol. 183:503–516, 1985.
5. Warwicker, J., Watson, H.C. Calculation of electric potential in the active site cleft due to α-helix dipoles. J. Mol. Biol. 157:671–679, 1982.
6. Rogers, N.K., Moore, G.R., Sternberg, M.J.E. Electrostatic interactions in globular proteins: Calculations of the pH dependence of the redox potential of cytochrome c_{551}. J. Mol. Biol. 182:613–616, 1985.
7. Warwicker, J., Ollis, D., Richards, F.M., Steitz, T.A. Electrostatic field of the large fragment of *Escherichia coli* DNA polymerase I. J. Mol. Biol 186:645–649, 1985.
8. Rogers, N.K., Sternberg, M.J. Electrostatic interactions in globular proteins. J. Mol. Biol. 174:527–542, 1984.
9. Zauher, R.J., Morgan, R.S. A new method for computing the macromolecular electric potential. J. Mol. Biol. 186:815-820, 1985.
10. Malinowski, D.P., Fridovich, I. Chemical modification of arginine at the active site of the bovine erythrocyte superoxide dismutase. Biochemistry 18:5909–5916, 1979.
11. Koppenol, W.H. In: "Oxygen and oxy-radicals in Chemistry and Biology." Rodgers, M.A.J., Powers, E.L. (eds). New York: Academic Press. 1981:671–674.
12. Cudd, A., Fridovich, I. Electrostatic interactions in the reaction mechanism of bovine erythrocyte superoxide dismutase. J. Biol. Chem. 257:11443–11447, 1982.
13. Getzoff, E.D., Tainer, J.A., Weiner, P.K., Kollman, P.A., Richardson, J.S., Richardson, D.S. Electrostatic recognition between superoxide and copper, zinc superoxide dismutase. Nature 306:287–290, 1983.
14. Allison, S.A., McCammon, J.A. Dynamics of substrate binding to copper, zinc superoxide dismutase. J. Phys. Chem. 89:1072–1074, 1985.
15. Allison, S.A., Ganti, G., McCammon, J. A. Simulation of the diffusion-controlled reaction between superoxide and superoxide dismutase. Biopolymers 24:1323–1336, 1985.
16. Burden, R.L., Faires, J.D. "Numerical Analysis." Boston: Prindle, Weber and Schmidt, 1985.
17. Jackson, J.D. "Classical Electrodynamics" (second edition). New York: John Wiley and Sons, 1975.
18. Connolly, M.L. Solvent-accessible surfaces of proteins and nucleic acids. Science 221:709–713, 1983.
19. Tainer, J.A., Getzoff, E.D., Beem, K.M., Richardson, J.S., Richardson, D.C. Determination and analysis of the 2 Å structure of copper, zine superoxide dismutase. J. Mol. Biol. 160:181–216, 1982.
20. Tainer, J.A., Getzoff, E.D., Richardson, J.S., Richardson, D.C. Structure and mechanism of copper, zinc superoxide dismutase. Nature 306:284–290, 1983.
21. Hagler, A.T., Huler, E., Lifson, S. Energy functions for peptide and proteins. J. Am. Chem. Soc. 96:5319–5327, 1974.
22. Berg, O.G., von Hippel, P.H. Diffusion controlled macromolecular interactions. Annu. Rev. Biophys. Biophys. Chem. 14:131–160, 1985.